



# Host-Guest Interactions Enhance the Performance of Viologen Electrolytes for Aqueous Organic Redox Flow Batteries

Aleksandr Korshunov<sup>+</sup><sup>[a]</sup>, Anna Gibalova<sup>+</sup><sup>[b]</sup>, Mariano Grünebaum,<sup>[c]</sup> Bart Jan Ravoo,<sup>\*[b]</sup> Martin Winter,<sup>\*[a, c]</sup> and Isidora Cekic-Laskovic<sup>\*[c]</sup>

Host-guest interactions are an attractive approach to design redox electrolytes, enabling to precisely tune the key properties for redox flow batteries such as half-cell redox potential, solubility, and stability. Herein we report a host-guest complex of highly water soluble (2-hydroxypropyl)- $\beta$ -cyclodextrin with 1-decyl-1'-ethyl-4,4'-bipyridinium dibromide as anolyte in a new aqueous organic redox flow battery (AORFB). The supramolecular anolyte ensured the total RFB voltage increase of  $\approx 9\%$  up to 0.97 V and provided a stable capacity delivery for more than 500 cycles with a capacity fade rate of 0.037%/cycle (2.84%/day) at high Coulombic ( $> 99.5\%$ ) and energy ( $> 62\%$ ) efficiencies. The results highlight host-guest interactions as promising strategy towards more effective storage of renewable energy within AORFBs.

The depletion of natural fossil deposits urges society to shift energy consumption needs towards renewable sources.<sup>[1]</sup> Despite the advantages of renewable energy harvesting such as theoretically unlimited supply and environmental friendliness, many practical challenges must be overcome to ensure a viable energy management. In light of this, the emerging aqueous organic redox flow battery (AORFB) technology is a promising solution for high scale stationary energy buffering ('peak shaving'), purporting to ensure sustainable continuous

energy delivery<sup>[2]</sup> and attracting a high research interest as benign substitution to 'all-metallic' analogues.<sup>[3]</sup>

Viologens<sup>[4]</sup> are well studied redox components among existing anolyte formulations for AORFBs.<sup>[5,6]</sup> Recent viologen anolyte advances commonly highlight synthetic modifications of redox structure, namely the quaternization of bipyridyl core with various substituents<sup>[7]</sup> or the  $\pi$ -conjugated structure extension,<sup>[8]</sup> which affect electrochemical properties of the resulting redox electrolytes and help to suppress secondary processes<sup>[9]</sup> like a radical dimerization leading to an undesired redox flow battery (RFB) capacity fading.<sup>[10]</sup> To further increase the performance of viologen anolytes alternative strategies are necessary.

Supramolecular chemistry is a field of chemistry which utilizes relatively weak interactions, such as electrostatic,  $\pi$ - $\pi$ , van der Waals or host-guest interactions.<sup>[11]</sup> A privileged place among host molecules is occupied by cyclodextrins – a family of bioengineered cyclic oligoglucosides obtained from sustainable resources. The hydrophobic effect is considered to be the main driving force of the host-guest complex formation of cyclodextrins in aqueous solution.<sup>[12]</sup> Electrochemistry of redox active materials like ferrocenes and viologens can be significantly affected by host-guest interactions,<sup>[13]</sup> resulting in a half-reaction potential shift<sup>[14]</sup> and an enhanced bulk stability of every redox state.<sup>[15]</sup>

Supporting electrolytes play an important role in RFB functioning by serving as auxiliary conductive media. Until now they have received only scarce attention mainly focused on solubility and compatibility issues.<sup>[16]</sup> To extend functionality of supporting electrolytes, highly water-soluble cyclodextrins, such as (2-hydroxypropyl)- $\beta$ -cyclodextrin (**HBCD**) can be employed to modulate the relevant physicochemical properties of RFB electrolytes and provide an increase of a power density and a lifespan of battery. In this communication we introduce an alternative strategy of an AORFB anolyte design featuring the ability of cyclodextrins to form host-guest complexes with surfactant viologens, employing the 1-decyl-1'-ethyl-4,4'-bipyridinium dibromide (**EDV**) complex with **HBCD** as redox active species (Figure 1). A key advantage of this supramolecular strategy is that essential components are simply mixed and elaborate synthetic modifications are avoided.

NMR titrations with an increasing amount of **HBCD** in aqueous 2 M KCl solution revealed the non-covalent molecular interactions between **EDV** and **HBCD** (Figures 2A and S4). Unambiguously assigned  $^1\text{H}$  NMR signals indicate the inclusion of the longer alkyl chain of **EDV** into the cavity of the

[a] A. Korshunov,<sup>+</sup> Prof. Dr. M. Winter  
MEET Battery Research Center  
University of Münster  
Corrensstrasse 46, 48149 Münster, Germany  
E-mail: martin.winter@uni-muenster.de

[b] A. Gibalova,<sup>+</sup> Prof. Dr. B. J. Ravoo  
Center for Soft Nanoscience and Organisch-Chemisches Institut  
University of Münster  
Busso-Peus-Straße 10, 48149 Münster, Germany  
E-mail: b.j.ravoo@uni-muenster.de

[c] Dr. M. Grünebaum, Prof. Dr. M. Winter, Dr. I. Cekic-Laskovic  
Helmholtz Institute Münster, IEK-12  
Forschungszentrum Jülich GmbH  
Corrensstrasse 46, 48149 Münster, Germany  
E-mail: i.cekic-laskovic@fz-juelich.de  
martin.winter@uni-muenster.de

[+] These authors contributed equally to this work.

Supporting information for this article is available on the WWW under  
<https://doi.org/10.1002/batt.202100018>

© 2021 The Authors. *Batteries & Supercaps* published by Wiley-VCH GmbH. This is an open access article under the terms of the Creative Commons Attribution License, which permits use, distribution and reproduction in any medium, provided the original work is properly cited.

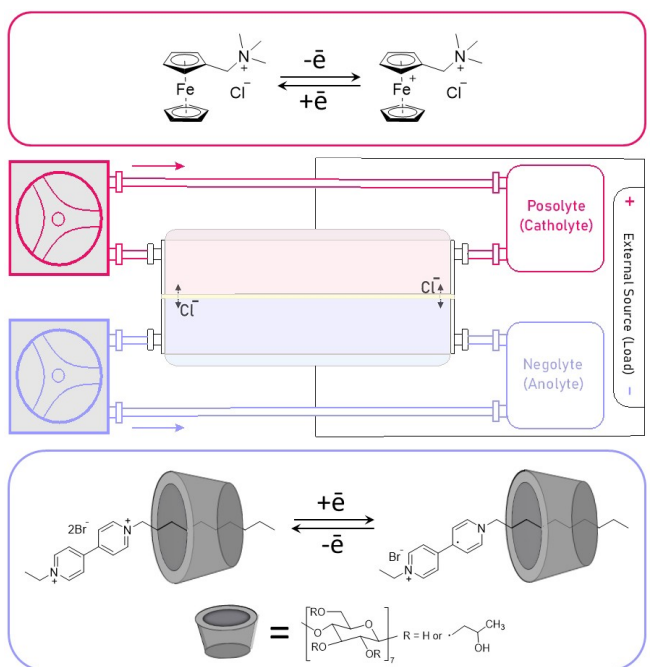


**Figure 1.** The scheme of AORFB setup. The anolyte system is an EDV-HBCD host-guest complex, the catholyte system is (ferrocenylmethyl) trimethylammonium chloride.

cyclodextrin, which causes a downfield shift on the terminal methyl group and methylene groups in vicinity to the bipyridine core. The estimated binding constant from NMR studies is  $K_a = 3.9 \cdot 10^3 \text{ M}^{-1}$ . Voltammetric studies on a planar electrode (Figure S5) as well as 'in flow' potentiodynamic bulk electrolysis ('in flow' cyclic voltammetry – CV)<sup>[17]</sup> of different EDV-HBCD anolytes (Figure 2B) confirmed that electrochemical characteristics of the first reduction process converge after exceeding the theoretical threshold of one HBCD equivalent. Consistent with the host-guest assembly, the gradual addition of HBCD resulted in negative half-reaction potential shift from  $-0.50 \text{ V}$  to  $-0.59 \text{ V}$  (vs. Ag|AgCl (sat.)), enhanced apparent 'in flow' heterogeneous kinetics (a decrease of overvoltages) and a smoother current distribution. Cotangent analysis – an 'in flow' potentiodynamic electrochemical impedance technique – is essentially complementary to the 'in flow' CV. The fundamental difference lies in the measured quantities: a cotangent of the phase angle at fixed frequency is recorded instead of the current. This technique allows to qualitatively assign main electrochemical phenomena for a given redox flow cell setup.<sup>[18]</sup> Thus, for potential regions of 'charging' I-II and 'discharging' III-IV (Figure 2C) the anolyte is predominantly affected by strong capacitive effects associated with a persistent positive charge of EDV existing for each redox state. Within the IV-V potential region the anolyte reaches a 'depletion' stage caused by a sharp increase of mass transfer impedance – the main reason of the incomplete capacity utilization of the RFBs. The observed cotangent peak splitting at the IV-V region is associated with a secondary convective mixing of the anolyte inside an electrolyte tank. The galvanostatic cycling of diluted EDV anolytes with different HBCD

content (Figure 2D) showed a similar trend. The gradual addition of HBCD stabilized the reproducibility of the mean discharge RFB voltage and gave a steady rise to the mean discharge voltage of the overbalanced RFB accordingly to 'in flow' CV experiments by average of 30 mV, 40 mV and 15 mV, respectively. Thus, the optimized composition of EDV AORFB anolyte included two equivalents of HBCD ( $E_{1/2} = -0.59 \text{ V}$  vs. Ag|AgCl (sat.)), which was used for further AORFB analysis.

Prototypes of AORFBs were equipped with the cyclodextrin-modified anolyte of higher concentration – 0.1 M EDV with 0.2 M HBCD, a 0.11 M (ferrocenylmethyl)trimethylammonium chloride (FCN, 0.39 V vs. Ag|AgCl (sat.)) catholyte<sup>[6]</sup> and a proper anion exchange membrane, providing the open theoretical battery voltage of 0.98 V (further details are provided in the Supporting Information (SI)). A 10% catholyte overbalancing enables to manage a battery solely over the anolyte half-cell. Each battery was exposed to an extended galvanostatic charge/discharge cycling procedure separated on three consecutive phases ('triathlon'): a cycling at various current densities, a long-term galvanostatic cycling and a anolyte stability analysis (Figure 3A).<sup>[19]</sup> This procedure aids to extract the relative properties of an RFB such as a current density dependency or a temporal bulk stability without disturbing a flow state of electrolytes.

Among the considered anion exchange membranes Selemion™ DSVN demonstrated the best performance in terms of energy delivery and general stability towards the considered redox electrolytes. Phase one (Figures 3B and 3C) revealed a low current density dependence and a high capacity utilization of the anolyte – 97.7% for the lowest and 77.5% for the highest current density applied with Coulombic efficiencies more than 99%. Thus, higher power densities are enabled for the RFB setup. Phase two (Figure 3A) suggested a decent charge/discharge cycling stability of the anolyte for 500 cycles with a cycling fading of 0.0372% (temporal – 2.84%/day) with an average energy efficiency of 63% (Figure S15a). The selected charge/discharge profiles (Figure 3D) are fairly reproducible, indicating no significant decrease of RFB performance. Corresponding anolyte potential profiles appear in the vicinity of the determined half-cell redox potential of  $-0.59 \text{ V}$  vs. Ag|AgCl (sat.). By the end of phase two, the residual volumetric energy density of the RFB was  $2.15 \text{ Ah L}^{-1}$  (80.2%). Phase three allowed to estimate the bulk electrolyte stability. The monitoring of an open circuit cell voltage (OCV) and an open circuit anolyte half-cell potential (OCP) during a circulation points at self-discharge process and electrolyte interactions at the interface with an RFB setup, especially with an electrolyte|membrane interface.<sup>[20]</sup> In case of the Selemion™ DSVN membrane (Figure 3E) the apparent charged and discharged states of the cyclodextrin-modified EDV anolyte showed a decay of 2.2% ( $\approx 60 \text{ mA h L}^{-1}$ ) and 1.5% ( $\approx 40 \text{ mA h L}^{-1}$ ), respectively, while other anion exchange membranes did not exhibit a similar consistent fading behavior, suggesting a strong dependence on membrane chemistry (Figures S12–S14).

To thoroughly address the RFB aging process, after completion of the 'triathlon' galvanostatic cycling procedure, the aged RFB was subjected to a stepwise discharge with full

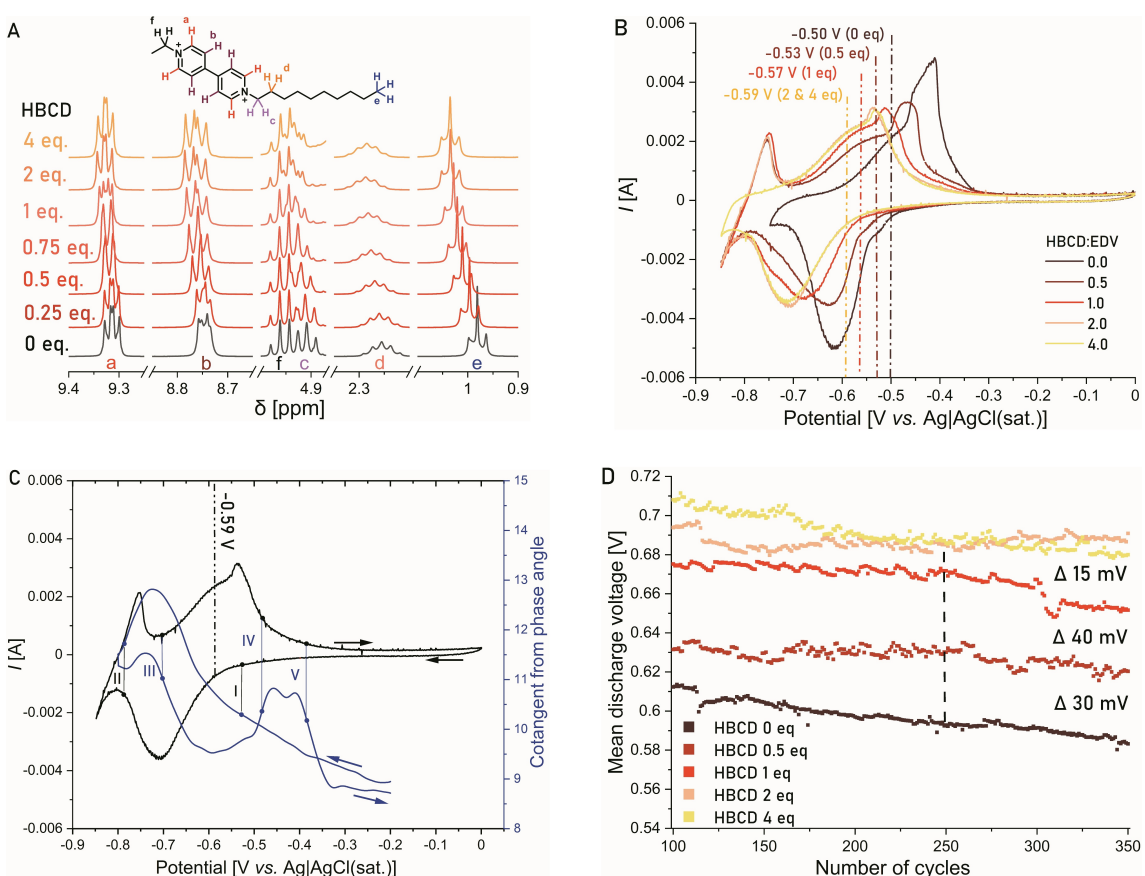


**Figure 2.** A)  $^1\text{H}$  NMR spectra of 15 mM EDV in 2 M KCl/D<sub>2</sub>O with different amount of HBCD added. B) Potentiodynamic bulk ‘in flow’ electrolysis of a 15 mM EDV anolyte with a different content of the HBCD additive (potential sweep rate 0.2 mV s<sup>-1</sup>). C) The correlation plot of ‘in flow’ potentiodynamic (0.2 mV s<sup>-1</sup>) bulk electrolysis and electrochemical impedance at a fixed frequency (700 Hz, the cotangent of phase angle representation) for a 15 mM EDV with 2 eq HBCD anolyte. D) A mean discharge voltage (100–350 cycles) of a 15 mM EDV|Fumasep® FAS-PET-130|0.15 M K<sub>4</sub>[Fe(CN)<sub>6</sub>] overbalanced redox flow battery with a different amount of HBCD additive.

cell galvanostatic electrochemical impedance spectra (G-EIS) analysis (Figure 4A). As the real part of the electrochemical impedance,  $\Omega_{re}$ , can be subdivided in a frequency-independent Ohmic and charge transfer part as well as a composition-and-frequency-dependent mass transfer part, this method helps to identify deviations from an ideal Nernstian behavior. The aged RFB did not show any serious deviations, affirming the viability of this prototype. The high frequency band  $\Omega_{re}$  values remained constant, confirming independency of the RFB setup from intermediate states of the redox electrolytes. For the low frequency band, minimal  $\Omega_{re}$  values emerged close to the theoretical battery cell open circuit voltage, while the rise of  $\Omega_{re}$  values at the early and late stages of discharge could be associated with mass transfer limitations.<sup>[21]</sup>

For the fresh anolyte, the simultaneously recorded open circuit anolyte half-cell redox potential and open circuit RFB voltage (OCP and OCV) for different states of the charge (Figure 4B) supported the previously identified half-cell potential of  $-0.59$  V vs. Ag|AgCl (sat.) and suggested a classical Nernstian behavior alike the prior G-EIS studies. As the catholyte had an excessive concentration of FCN, the OCPs for the charging process covered intermediate states, where the second electron reduction of viologen proceeds. The OCV

values suggested a practical RFB voltage of 0.97 V, which was slightly below the theoretical value of 0.98 V. This small discrepancy can be presumably referred to specifics of the half-cell potential determination and imperfections of reference electrodes.<sup>[22]</sup> Starting from the corresponding to state of charge OCP value, a set of ‘in flow’ linear sweep voltammograms shows a detailed anolyte current response to a potential sweep under hydrodynamic flow conditions. The apparent symmetry of resultant charge (Figure 4C) and discharge (Figure 4D) mappings suggested a bulk electrochemical reversibility of the cyclodextrin-modified anolyte. The difference between the observed maximum current values and a positive overpotential of  $\approx 15$  mV for 50% state of charge indicate a slightly inferior electrochemical behavior of the anolyte upon a discharge process.

In summary, the modification of the supporting electrolyte with water-soluble cyclodextrin HBCD enhances the battery relevant characteristics of the pH neutral aqueous viologen EDV anolyte. The anolyte half-cell potential shifts from  $-0.50$  V to  $-0.59$  V (vs. Ag|AgCl (sat.)) and the bulk electrolyte stability at different states of charge supports a nearly 9% increase of the prototype AORFB voltage and battery cell operation for more than 500 cycles with a capacity fade rate of 0.037%/cycle

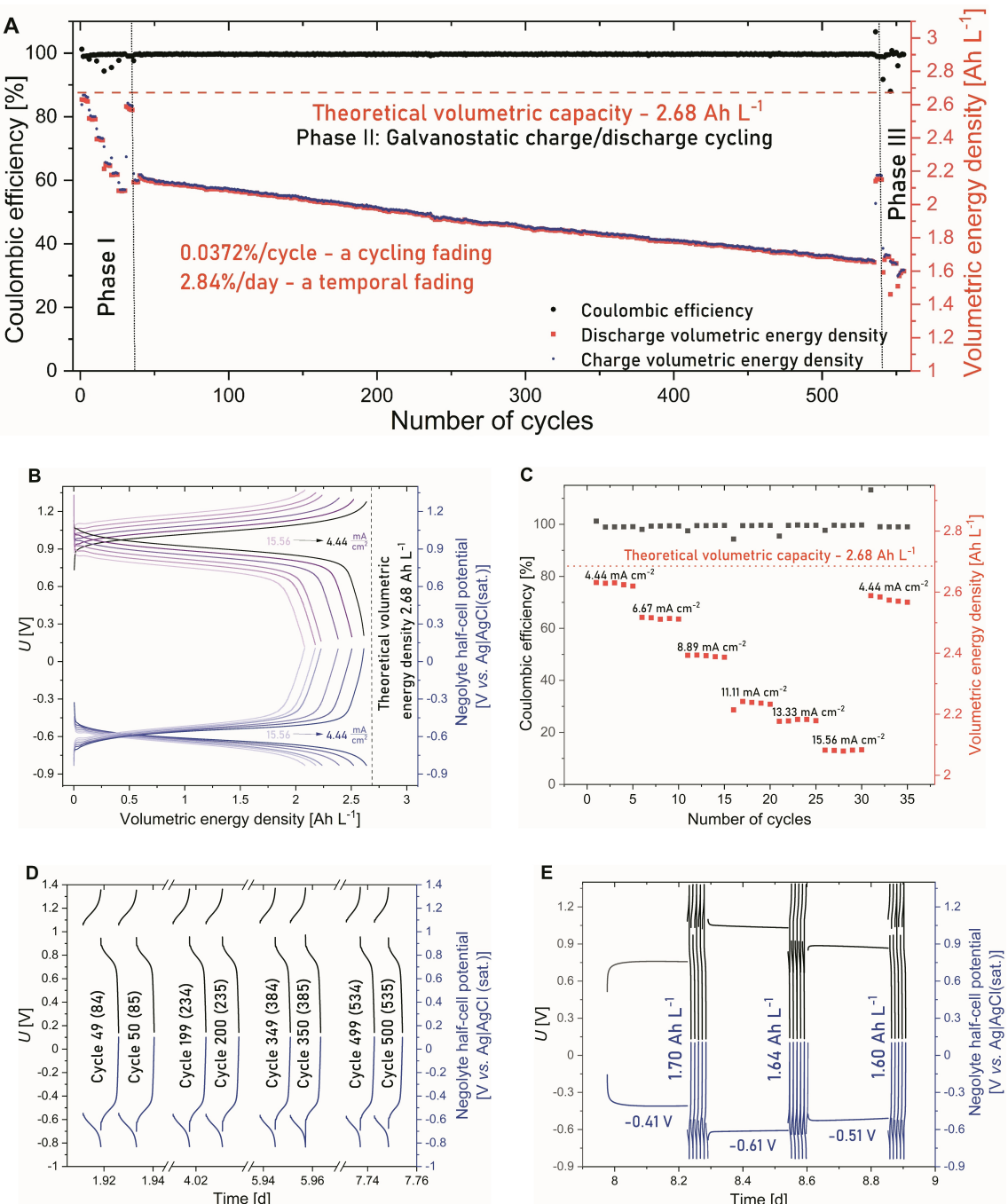


**Figure 3.** Galvanostatic cycling performance in a 0.1 M EDV + 0.2 M HBCD | Slemion™ DSVN (anion exchange membrane) | 0.11 M FCN redox flow battery. A) A general overview on a charge/discharge procedure subdivided on three consecutive stages. Phase I: the current density test, phase II: galvanostatic charge/discharge cycling ( $13.33 \text{ mA cm}^{-2}$ ), phase III: a stability analysis. B) Phase I. Galvanostatic charge/discharge profiles at various current densities (4.44, 6.67, 8.89, 11.11, 13.33, 15.56  $\text{mA cm}^{-2}$ ) recorded with an anolyte half-cell potential management. C) Phase I. Discharge volumetric energy densities and corresponding Coulombic efficiencies at various current densities. D) Phase II. Voltage and anolyte half-cell potential (vs. Ag|AgCl(sat.)) profiles: a time evolution of the charge/discharge profiles. E) Phase III. The stability analysis: open circuit anolyte half-cell redox potential (vs. Ag|AgCl(sat.)) and OCV monitoring and a galvanostatic cycling ( $13.33 \text{ mA cm}^{-2}$ , 5 cycles with alternating end charging and discharging).

(2.84%/day) and an average discharge energy density of  $1.399 \text{ Wh L}^{-1}$  (a theoretical value of energy density –  $2.599 \text{ Wh L}^{-1}$ ). To our knowledge, the utilization of specific host-guest interactions has not been previously employed for RFB anolytes. The concept of non-covalent interactions proved to be an effective basis for the alternative flow battery strategy,

implying the extended functionality of RFB supporting electrolytes. The development of redox active host guest complexes is considered as a key step towards new advanced supramolecular redox electrolytes which can be made simply by mixing components rather than deploying elaborated chemical synthesis. The presented research introduces non-

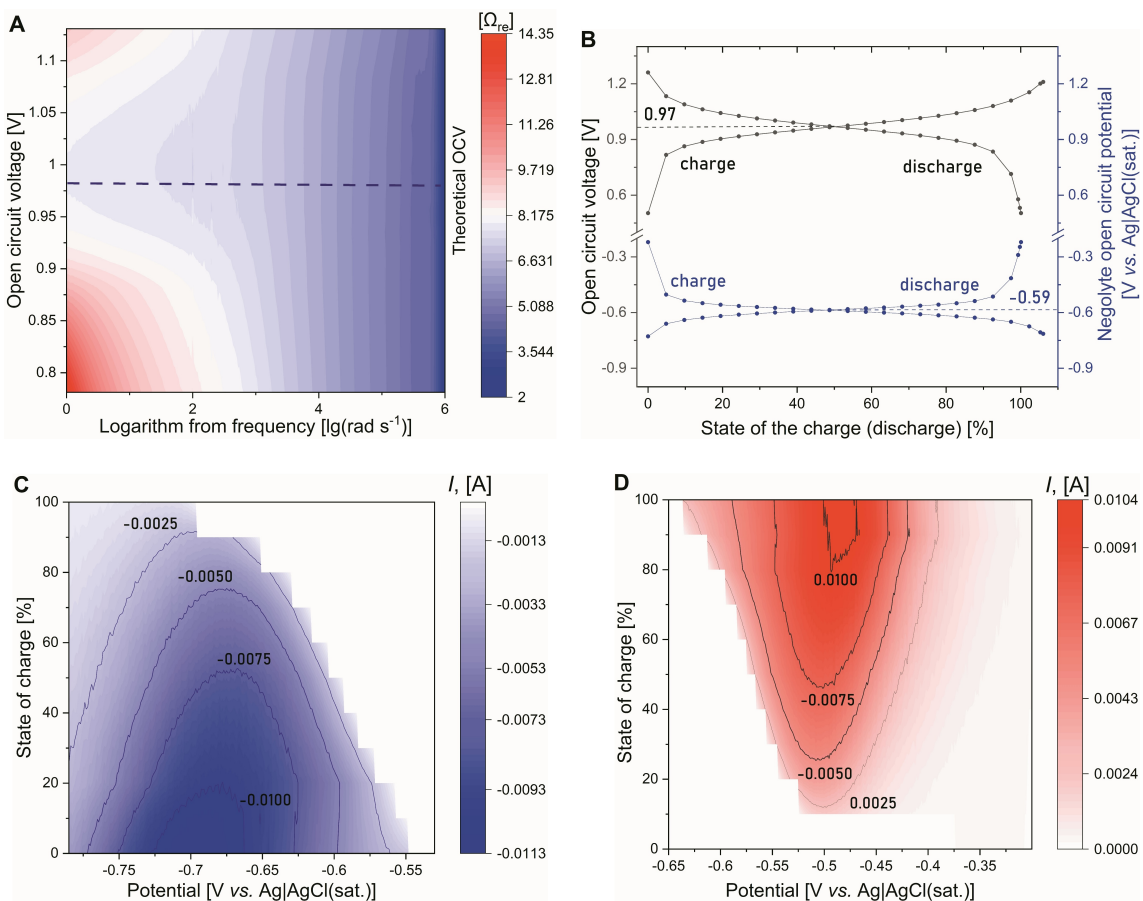


**Figure 4.** The state of charge studies of a 0.1 M EDV + 0.2 M HBCD | Selemion™ DSVN | 0.11 M FCN RFB: A) A map representation of the real part of galvanostatic (DC = 0 A) impedance spectra upon a stepwise discharge of the aged RFB vs. the open circuit cell voltage and applied AC frequency. B) Open circuit cell voltage (black) and anolyte open circuit half-cell potential (blue) vs. state of charge dependency. C) 'In flow' linear sweep voltammograms of the anolyte upon a stepwise charge (cathodic scan, a potential scan rate 0.2 mV s<sup>-1</sup>, end scan point -0.8 V vs. Ag|AgCl (sat.)) vs. a state of charge. D) 'In flow' linear sweep voltammograms of the anolyte upon a stepwise discharge (anodic scan, a potential scan rate 0.2 mV s<sup>-1</sup>, end scan point -0.3 V vs. Ag|AgCl (sat.)) vs. a state of charge.

covalent interactions as a powerful tool for developing of the benign electrolyte materials for AORFBs.

## Acknowledgements

We thank the Ministry of Economic Affairs, Innovation, Digitalization and Energy of the State of North Rhine-Westphalia for funding this research work in the frame of the "GrEEn" project (313-W044A) and the Deutsche Forschungsgemeinschaft (DFG) for funding through the SFB 858. Open access funding enabled and organized by Projekt DEAL.

## Conflict of Interest

The authors declare no conflict of interest.

**Keywords:** Electrochemistry · host-guest systems · redox flow battery · cyclodextrins · viologen

- [1] a) S. Dühnen, J. Betz, M. Kolek, R. Schmuck, M. Winter, T. Placke, *Small Methods* **2020**, *4*, 2000039; b) M. Winter, B. Barnett, K. Xu, *Chem. Rev.* **2018**, *118*, 11433; c) R. Schmuck, R. Wagner, G. Höppl, T. Placke, M. Winter, *Nat. Energy* **2018**, *3*, 267; d) R. M. Darling, K. G. Gallagher, J. A. Kowalski, S. Ha, F. R. Brushett, *Energy Environ. Sci.* **2014**, *7*, 3459.
- [2] a) P. Alotto, M. Guarneri, F. Moro, *Renewable Sustainable Energy Rev.* **2014**, *29*, 325; b) L. F. Arenas, C. Ponce de León, F. C. Walsh, *Curr. Opin. Electrochem.* **2019**, *16*, 117; c) G. Kear, A. A. Shah, F. C. Walsh, *Int. J. Energy Res.* **2012**, *36*, 1105; d) A. Lucas, S. Chondrogiannis, *Int. J. Electr. Power Energy Syst.* **2016**, *80*, 26.
- [3] a) X. Wei, W. Pan, W. Duan, A. Hollas, Z. Yang, B. Li, Z. Nie, J. Liu, D. Reed, W. Wang et al., *ACS Energy Lett.* **2017**, *2*, 2187; b) Y. Ding, C. Zhang, L. Zhang, Y. Zhou, G. Yu, *Chem. Soc. Rev.* **2018**, *47*, 69; c) Y. Ding, Y. Li, G. Yu, *Chem* **2016**, *1*, 790; d) S. Jin, Y. Jing, D. G. Kwabi, Y. Ji, L. Tong, D. de Porcellinis, M.-A. Goulet, D. A. Pollack, R. G. Gordon, M. J. Aziz, *ACS Energy Lett.* **2019**, *4*, 1342.
- [4] L. Striepe, T. Baumgartner, *Chem. Eur. J.* **2017**, *23*, 16924.
- [5] a) J. Luo, B. Hu, M. Hu, Y. Zhao, T. L. Liu, *ACS Energy Lett.* **2019**, *4*, 2220; b) J. Winsberg, T. Hagemann, T. Janoschka, M. D. Hager, U. S. Schubert, *Angew. Chem. Int. Ed.* **2017**, *56*, 686; *Angew. Chem.* **2017**, *129*, 702; c) K. Lin, Q. Chen, M. R. Gerhardt, L. Tong, S. B. Kim, L. Eisenach, A. W. Valle, D. Hardee, R. G. Gordon, M. J. Aziz, M. P. Marshak, *Science* **2015**, *349*, 1529; d) D. G. Kwabi, K. Lin, Y. Ji, E. F. Kerr, M.-A. Goulet, D. de Porcellinis, D. P. Tabor, D. A. Pollack, A. Aspuru-Guzik, R. G. Gordon, M. J. Aziz, *Joule* **2018**, *2*, 1894; e) W. Lee, A. Permatasari, Y. Kwon, *J. Mater. Chem. C* **2020**, *8*, 5727.
- [6] V. Singh, S. Kim, J. Kang, H. R. Byon, *Nano Res.* **2019**, *12*, 1988.

- [7] a) E. S. Beh, D. de Porcellinis, R. L. Gracia, K. T. Xia, R. G. Gordon, M. J. Aziz, *ACS Energy Lett.* **2017**, *2*, 639; b) Y. Liu, Y. Li, P. Zuo, Q. Chen, G. Tang, P. Sun, Z. Yang, T. Xu, *ChemSusChem* **2020**, *13*, 2245; c) Y. Lv, Y. Liu, T. Feng, J. Zhang, S. Lu, H. Wang, Y. Xiang, *J. Mater. Chem. A* **2019**, *7*, 27016; d) T. Janoschka, C. Friebe, M. D. Hager, N. Martin, U. S. Schubert, *ChemistryOpen* **2017**, *6*, 216.
- [8] J. Luo, B. Hu, C. Debruler, T. L. Liu, *Angew. Chem. Int. Ed.* **2018**, *57*, 231; *Angew. Chem.* **2018**, *130*, 237.
- [9] D. G. Kwabi, Y. Ji, M. J. Aziz, *Chem. Rev.* **2020**, *120*, 6467.
- [10] a) B. Hu, Y. Tang, J. Luo, G. Grove, Y. Guo, T. L. Liu, *Chem. Commun.* **2018**, *54*, 6871; b) M. R. Geraskina, A. S. Dutton, M. J. Juetten, S. A. Wood, A. H. Winter, *Angew. Chem. Int. Ed.* **2017**, *56*, 9435; *Angew. Chem.* **2017**, *129*, 9563.
- [11] J.-M. Lehn, *European Review* **2009**, *17*, 263.
- [12] a) S. Engel, N. Möller, B. J. Ravoo, *Chem. Eur. J.* **2018**, *24*, 4741; b) B. V. K. J. Schmidt, C. Barner-Kowollik, *Angew. Chem. Int. Ed.* **2017**, *56*, 8350; *Angew. Chem.* **2017**, *129*, 8468.
- [13] a) A. Mirzoian, A. E. Kaifer, *Chem. Eur. J.* **1997**, *3*, 1052; b) C. L. Young-mi Lee, *Bull. Korean Chem. Soc.* **1999**, *20*; c) C. A. Nijhuis, B. A. Boukamp, B. J. Ravoo, J. Huskens, D. N. Reinhoudt, *J. Phys. Chem. C* **2007**, *111*, 9799; d) C. A. Nijhuis, B. J. Ravoo, J. Huskens, D. N. Reinhoudt, *Coord. Chem. Rev.* **2007**, *251*, 1761; e) Y. Li, Z. Xu, Y. Liu, S. Jin, E. M. Fell, B. Wang, R. G. Gordon, M. J. Aziz, Z. Yang, T. Xu, *ChemSusChem* **2020**, DOI: 10.1002/cssc.202002516.
- [14] Y. Zheng, A. E. Kaifer, *ChemElectroChem* **2019**, *6*, 5610.
- [15] B. Tang, J. Zhao, J.-F. Xu, X. Zhang, *Chem. Sci.* **2020**, *11*, 1192.
- [16] a) R. Chen, *ChemElectroChem* **2019**, *6*, 603; b) X. Wei, W. Xu, J. Huang, L. Zhang, E. Walter, C. Lawrence, M. Vijayakumar, W. A. Henderson, T. Liu, L. Cosimescu et al., *Angew. Chem. Int. Ed.* **2015**, *54*, 8684; *Angew. Chem.* **2015**, *127*, 8808.
- [17] A. Korshunov, M. J. Milner, M. Grünebaum, A. Studer, M. Winter, I. Cekic-Laskovic, *J. Mater. Chem. A* **2020**, *8*, 22280.
- [18] A. Battistel, G. Du, F. La Mantia, *Electroanalysis* **2016**, *28*, 2346.
- [19] F. R. Brushett, M. J. Aziz, K. E. Rodby, *ACS Energy Lett.* **2020**, *5*, 879.
- [20] a) J. Sun, D. Shi, H. Zhong, X. Li, H. Zhang, *J. Power Sources* **2015**, *294*, 562; b) M. Abdul Aziz, K. Oh, S. Shanmugam, *Chem. Commun.* **2017**, *53*, 917.
- [21] A. Lasia, *Electrochemical impedance spectroscopy and its applications*, Springer, New York, **2014**, pp. 100–101.
- [22] A. Bott, *Curr. Sep.* **1995**, *14*, 64–69.

---

 Manuscript received: January 19, 2021

Revised manuscript received: February 3, 2021

Version of record online: February 11, 2021